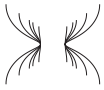
JGSP **51** (2019) 41–71

JOURNAL OF
Geometry and Symmetry in Physics
ISSN 1312-5192

EXPLICIT DESCRIPTION OF SOME CLASSES OF NON-BENDING SURFACES

VLADIMIR I. PULOV AND IVAÏLO M. MLADENOV

Presented by Ivaïlo M. Mladenov

Abstract. Here we consider a family of axially symmetric surfaces modeling the shape of thin mechanical shells that are deformable without bending under uniform loading. With the exception of very few surfaces, like the well known right circular cylinder and the sphere, the surfaces of this family have no closed form description in elementary functions. Our main goal is to present their explicit parameterizations including both classes of open and closed families. We distinguish four classes of non-bending surfaces differing by their canonical representations using the normal elliptic integrals and the Jacobian elliptic functions.

MSC: 74K25, 74A10, 53A04, 53A05, 33E05
Keywords: Axially symmetric surfaces, bending of shells, elliptic integrals, parameterizations, stress analysis, surface geometry

Contents

List of Symbols

(OX, OY, OZ)	Cartesian coordinate system in $\mathbb{R}^3$
(x, y, z)	Cartesian coordinates
$\mathcal{S}$	surface in the three-dimensional space
$(x(u,v), y(u,v), z(u,v))$	parameterization of the surface $\mathcal{S}$
(OX, OZ)	Cartesian coordinate system in $\mathbb{R}^2$
(x, z)	Cartesian coordinates in the plane
$(x_j(u), z_j(u))$	parameterization of the profile curves of the non-bending surfaces of class $j = 1, 2, 3, 4$
$a, c \in \mathbb{R}$	parameters (constants of integration)
$\nu \in \mathbb{R}$	parameter of the non-bending surfaces
N, S	North and South Poles of closed surfaces
E	Equator
κ_μ, κ_π	meridional and parallel curvatures
$\mathcal{R}_\mu, \mathcal{R}_\pi$	meridional and parallel radii
r	radius of the basic parallel circle
$P(t)$	quadratic polynomial
$\mathcal{D}$	discriminant of $P(t)$
σ, τ	roots of $P(t)$
σ_j, τ_j	roots of $P(t)$ related to the non-bending surfaces of class j
θ	angular coordinate of the parallel circle
ϕ	angular coordinate of the meridians
$\mathbf{n}, \mathbf{n}_\theta, \mathbf{n}_\phi$	unit vectors along the normal, meridional and parallel directions
k	modulus of the elliptic function
k_j	modulus of the elliptic function related to the non-bending surfaces of class j
$\mathrm{am}(u,k)$	Jacobian amplitude function
$\Delta(\varphi) = \sqrt{1 - k^2 \sin^2\varphi}$	delta function
$\mathrm{sn}(u,k), \mathrm{cn}(u,k), \mathrm{dn}(u,k)$	Jacobian elliptic functions
$\mathrm{sn}^{-1}(u,k), \mathrm{cn}^{-1}(u,k), \mathrm{dn}^{-1}(u,k)$	inverse Jacobian elliptic functions
$F(\varphi,k), E(\varphi,k)$	elliptic integrals of the first and second kind
$K(k), E(k)$	complete elliptic integrals of the first and second kind
$\Pi(\varphi,n,k), \Pi(n,k)$	incomplete and complete elliptic integrals of the third kind

1. Introduction

We are interested in the so called *non-bending surfaces* of revolution. Such surfaces are most often referred to the middle surfaces of axially symmetric shells (e.g., pressure vessels, tanks, air-supported envelopes), deforming under evenly distributed loads without bending, which means that in the process of deformation the normal at any point of the shell's surface preserves its direction. One should notice that this geometrical definition is quite different from the analytical one explored in the classical differential geometry (see [9] and the Comments section at the end of the present paper).

Using the *membrane shells theory* [5, 16], i.e., disregarding all bending and twisting moments, Gurevich and Kalinin [7] have derived the *non-bending condition* in the form

$$(3-\frac{\mathcal{R}_\pi}{\mathcal{R}_\mu})\frac{\mathrm{d}\mathcal{R}_\pi}{\mathrm{d}\theta}-\mathcal{R}_\pi\frac{\mathrm{d}}{\mathrm{d}\theta}(\frac{\mathcal{R}_\pi}{\mathcal{R}_\mu})=0$$

in which $\mathcal{R}_\pi$ and $\mathcal{R}_\mu$ are the curvatures radii and θ is the angle between the normal to the middle surface and the axis of revolution (Fig. 1).

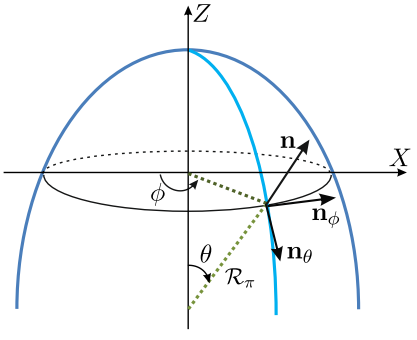

Figure 1. A sketch of a typical surface of revolution.

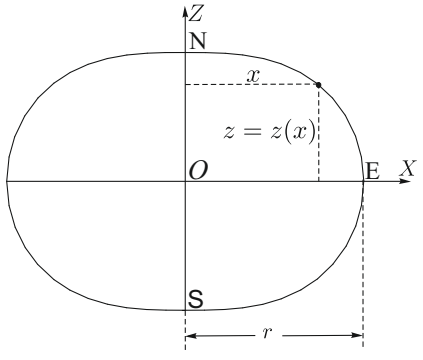

Figure 2. A typical closed profile curve in XOZ-plane.

Rewriting the above equation in terms of the principle curvatures κ_μ and κ_π we have respectively

$$\frac{3\kappa_\pi-\kappa_\mu}{\kappa_\pi^2}\cdot\frac{\mathrm{d}\kappa_\pi}{\mathrm{d}\theta}+\frac{\mathrm{d}}{\mathrm{d}\theta}\left(\frac{\kappa_\mu}{\kappa_\pi}\right)=0. \tag{1}$$

Elaborating a little bit further we have also

$$\frac{3}{\kappa_\pi}\cdot\frac{\mathrm{d}\kappa_\pi}{\mathrm{d}\theta}+\kappa_\mu\frac{\mathrm{d}}{\mathrm{d}\theta}\left(\frac{1}{\kappa_\pi}\right)+\frac{\mathrm{d}}{\mathrm{d}\theta}\left(\frac{\kappa_\mu}{\kappa_\pi}\right)=0$$

which after a multiplication by $1/\kappa_\pi$ can be rewritten finally as

$$\frac{\mathrm{d}}{\mathrm{d}\theta}\left(\frac{\kappa_\mu}{\kappa_\pi^2}-\frac{3}{\kappa_\pi}\right)=0.$$

The last identity actually means that the relation

$$\kappa_\mu = 2a\kappa_\pi^2 + 3\kappa_\pi \tag{2}$$

in which a is a real constant is a first integral of the equation (1). Speaking geometrically we should say that we have to deal with Weingarten surfaces [6, 8, 11, 12, 18, 21] which obey in the present case to a quadratic relationship between κ_μ and κ_π.

Let the surface $\mathcal{S}$ under consideration is generated by the rotation of a plane curve γ (profile curve) about the OZ-axis of some orthogonal (OX, OY, OZ) coordinate system in $\mathbb{R}^3$. We assume that $\mathcal{S}$ intersects the XOY-plane at right angle $\theta = \pi/2$ and the profile curve γ lies in the XOZ-plane. Let this curve γ is specified by the function $z = z(x)$ of the radial coordinate $x \geq 0$, which is chosen in such a way that $z(r) = 0$, for some positive number r (see Fig. 2). The curve on the surface traced by this point (the point $(r, 0)$ of the profile curve) is called the *basic parallel circle* or the *equator* of $\mathcal{S}$ for which we assume that it has a predetermined (fixed) radius r. In these settings the principal curvatures κ_π and κ_μ are given by the formulas [17]

$$\kappa_\pi = \frac{\dot{z}(x)}{x\sqrt{1+\dot{z}^2(x)}}, \qquad \kappa_\mu = \frac{\mathrm{d}(x\kappa_\pi)}{\mathrm{d}x}, \qquad x \geq 0 \tag{3}$$

where $\dot{z}(x) \equiv \mathrm{d}z(x)/\mathrm{d}x$.

In expanded form the second equation can be written equivalently as [13, p. 154]

$$\frac{\mathrm{d}\kappa_\pi}{\mathrm{d}x} = \frac{\kappa_\mu - \kappa_\pi}{x}. \tag{4}$$

The substitution of κ_μ from (2) into the above equation produces

$$\left(\frac{1}{\kappa_\pi} - \frac{a}{a\kappa_\pi + 1}\right)\mathrm{d}\kappa_\pi = 2\frac{\mathrm{d}x}{x}$$

which can be immediately integrated giving us the explicit expression for the parallel curvature in the form in which c is a new integration constant

$$\kappa_\pi = \frac{x^2}{c - ax^2}. \tag{5}$$

Relying on (4) one can find as well the meridional curvature

$$\kappa_\mu = \frac{(3c - ax^2)x^2}{(c - ax^2)^2}. \tag{6}$$

Due to the axial symmetry, the principal curvatures (respectively the principal radii of the curvatures $\mathcal{R}_\pi$ and $\mathcal{R}_\mu$) at the points of a given parallel circle (for a given angle θ) are the same. Based on this observation and the assumptions made earlier, we can introduce the parameter ν defined as the ratio between the two principal radii of curvature $\mathcal{R}_\pi(\pi/2)$ and $\mathcal{R}_\mu(\pi/2)$ on the basic parallel circle (for $\theta = \pi/2$)

$$\nu = \frac{\mathcal{R}_\pi(\pi/2)}{\mathcal{R}_\mu(\pi/2)} = \frac{r}{\mathcal{R}_\mu(\pi/2)}.$$

Recall, that the curvature and the radius of curvature are reciprocal quantities, and that $\mathcal{R}_\pi(\pi/2) = r$. Then, by a straightforward substitution in (2) and (5), one can deduce the relations

$$a = \frac{(\nu - 3)r}{2}, \qquad c = \frac{(\nu - 1)r^3}{2}, \qquad \nu \in \mathbb{R}. \tag{7}$$

On substituting for a with the expression just obtained the quadratic Weingarten relation (2) takes the form

$$\kappa_\mu = (\nu - 3)r\kappa_\pi^2 + 3\kappa_\pi. \tag{8}$$

Three of the surfaces obeying the above condition can be immediately recognized. These are the right circular cylinder for $\nu = 0$, the sphere for $\nu = 1$ (both having the same constant parallel curvatures, $\kappa_\pi(\theta) \equiv 1/r$, $\theta \in [-\pi/2, \pi/2]$), and the rotational surface for $\nu = 3$, best known as the *LW*(2) *balloon*. With the exception of three of the surfaces – the sphere, the right circular cylinder and the surface obtained for $\nu = 9$ (see below), that are parameterizable through elementary functions, the condition (8) defines surfaces which can not be described by means only of the elementary functions. One such surface is the above mentioned *LW*(2) balloon. The *LW*(2) balloon satisfies the relation $\kappa_\mu = 3\kappa_\pi$, and therefore belongs to the special class of linear Weingarten *LW*(*n*) *surfaces* (for relevant definitions and details see [19]).

Relying on numerical calculations Gurevich and Kalinin [7] (see also [10, p. 150]) have shown that the considered class of non-bending surfaces can be divided into two subclasses of closed and open "at the top" surfaces. Closed surfaces are obtained for $\nu \geq 1$ and the open ones for $\nu < 1$ (in our notation).

In what follows our principle aim will be to derive explicit parameterizations of

all non-bending surfaces whose principal curvatures satisfy the quadratic relationship (8) (compare with [20] where only the closed surfaces have been described explicitly).
Looking at the problem from the abstract point of view one can refer to the fundamental existence and uniqueness theorem in the theory of plane curves which states that a curve is uniquely determined up to rigid motion by its curvature and try to follow the recepies described elsewhere, see [13] and [2,3]. Instead, we will take advantage of the fact that the principal curvatures κ_π is also at our disposition and relying on some simple geometrical arguments one ends with the formula

$$z(x) = \pm \int \frac{x\kappa_\pi(x)\mathrm{d}x}{\sqrt{1 - x^2\kappa_\pi^2(x)}}. \tag{9}$$

Further, by making use of the expression for $\kappa_\pi(x)$ given in the equation (5) and taking into account the definition of the parameter ν, i.e., $\kappa_\mu(r)/\kappa_\pi(r) \equiv \nu$ the above integral beccomes

$$z(\chi) = \pm\, r \int_\chi^1 \frac{t\mathrm{d}t}{\sqrt{(1-t)\left(4t^2 - (\nu-1)(\nu-5)t + (\nu-1)^2\right)}}, \qquad \chi = \frac{x^2}{r^2} \tag{10}$$

in which the plus sign refers for the surfaces lying inside the cylinder $\nu = 0$

$$x \in [0, r], \qquad \chi \in [0, 1], \qquad t \in (0, 1) \tag{11}$$

and the minus sign for the surfaces that are positioned outside of the cylinder

$$x \in [r, +\infty), \qquad \chi \in [1, +\infty), \qquad t \in (1, +\infty). \tag{12}$$

For $\nu = 1$ and $\nu = 9$ the quadratic polynomial

$$P(t) = 4t^2 - (\nu-1)(\nu-5)t + (\nu-1)^2 \tag{13}$$

has multiple roots so that the integral (10) can be evaluated in terms of elementary functions, and in this situation two non-bending surfaces are immediately obtained: the sphere for $\nu = 1$, and the surface for $\nu = 9$ which generating curve $\gamma(x) = (x, 0, z(x))$, (the upper part, $z(x) \geq 0$, for $x \in [-r, r]$) is given by the formula

$$\gamma(u) = \left(r\sin u,\ 0,\ \frac{r}{2}\Big(\frac{8}{\sqrt{3}}\arctan\frac{\cos u}{\sqrt{3}} - 2\cos u\Big)\right), \qquad u \in [-\pi/2, \pi/2]\,.$$

When the roots of the polynomial under the radical are simple ones (not multiple), which is fulfilled when ν is not equal to one or nine, the above integral belongs to the class of non-elementary *elliptic integrals*. Our present goal is to build up the canonical forms of the elliptic integral (10) for all the values of the parameter $\nu \in [-\infty, +\infty]$.

2. Reduction to the Canonical Forms

As it was first shown by Legendre (1811-1819), the elliptic integrals are always reducible to their *canonical form*, which means that they are expressible as a linear combination of elementary functions and the three fundamental elliptic integrals – the so called *normal elliptic integrals* of the first

$$F(\varphi, k) \equiv \int\limits_0^{\zeta} \frac{\mathrm{d}t}{\sqrt{(1-t^2)(1-k^2t^2)}} = \int\limits_0^{\varphi} \frac{\mathrm{d}\theta}{\sqrt{1-k^2\sin^2\theta}} \tag{14}$$

respectively the second

$$E(\varphi, k) \equiv \int\limits_0^{\zeta} \sqrt{\frac{1-k^2t^2}{1-t^2}}\mathrm{d}t = \int\limits_0^{\varphi} \sqrt{1-k^2\sin^2\theta}\,\mathrm{d}\theta \tag{15}$$

and the third kind

$$\Pi(\varphi, n, k) \equiv \int\limits_0^{\zeta} \frac{\mathrm{d}t}{(1-nt^2)\sqrt{(1-t^2)(1-k^2t^2)}} = \int\limits_0^{\varphi} \frac{\mathrm{d}\theta}{(1-n\sin^2\theta)\sqrt{1-k^2\sin^2\theta}}\cdot \tag{16}$$

These three standard elliptic integrals depend on the variable upper limit ζ or φ, which is considered as their *argument*

$$\zeta = \sin\varphi, \qquad \zeta \in (0, 1], \qquad \varphi \in (0, \frac{\pi}{2}]$$

and the so called *elliptic modulus* $k \in (0,1)$, while the third one depends on one additional *parameter* for which it is assumed that $n \neq 1$ and $n \neq k^2$ (for more details about the elliptic integrals, see e.g. [1]).

In order to reduce the elliptic integral (10) to its canonical form we will make substitutions involving Jacobian elliptic functions. The method dates back to Abel (1827-1828) and Jacobi (1828) who almost simultaneously suggested to consider the inversion of the integrals

$$u = F(\varphi, k) \equiv \int_0^{\zeta} \frac{\mathrm{d}t}{\sqrt{(1-t^2)(1-k^2t^2)}} = \int_0^{\varphi} \frac{\mathrm{d}\theta}{\sqrt{1-k^2\sin^2\theta}}$$

as new functions which are called respectively am (*amplitude*) and sn (*sine amplitude*)

$$\varphi = \mathrm{am}(u,k), \qquad \zeta = \sin\varphi = \mathrm{sn}(u,k). \tag{17}$$

Two related functions cn (*cosine amplitude*) and dn (*delta amplitude*) were introduced via the formulas

$$\Delta\varphi = \sqrt{1-k^2\sin^2\varphi}, \quad \mathrm{cn}(u,k) = \sqrt{1-\zeta^2} = \cos\varphi, \quad \mathrm{dn}(u,k) = \sqrt{1-k^2\zeta^2}. \tag{18}$$

The functions $\mathrm{sn}(u,k)$, $\mathrm{cn}(u,k)$ and $\mathrm{dn}(u,k)$ are called *Jacobian elliptic functions*. Their modern notation is due to Gudermann (1838). Assuming the modulus k to be fixed we will simply write $\varphi = \mathrm{am}\, u$, etc. We find it useful to visualize the

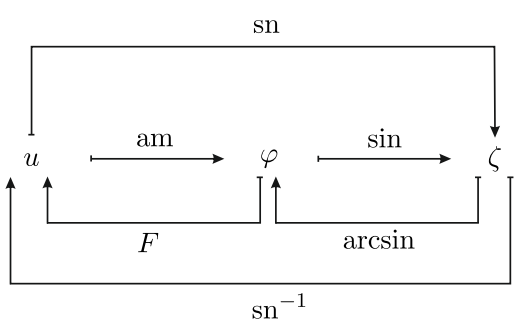

Figure 3. Commutative diagram for the inversion of the normal elliptic integral of the first kind.

composite functions by commutative "barred arrow diagrams" as the one displayed in Fig. 3.

As a consequence of the above formulas the following fundamental relations between the Jacobian elliptic functions are obtained

$$\mathrm{sn}^2 u + \mathrm{cn}^2 u = 1, \qquad \mathrm{dn}^2 u + k^2 \mathrm{sn}^2 u = 1, \qquad \mathrm{dn}^2 u - k^2 \mathrm{cn}^2 u = 1 - k^2 \quad (19)$$

and the representations of the normal elliptic integrals via the amplitude function or the Jacobian elliptic functions are easily revealed

$$F(\varphi, k) \,=\, F(\mathrm{am}\, u, k) \equiv u = \int\limits_0^u \mathrm{d}\tilde{u} \tag{20}$$

$$E(\varphi, k) \,=\, E(\mathrm{am}\, u, k) = \int\limits_0^u \mathrm{dn}^2 \tilde{u} \mathrm{d}\tilde{u} \tag{21}$$

$$\Pi(\varphi, n, k) \,=\, \Pi(\mathrm{am}\, u, n, k) = \int\limits_0^u \frac{\mathrm{d}\tilde{u}}{1 - n\mathrm{sn}^2 \tilde{u}}. \tag{22}$$

The derivatives of the Jacobian elliptic functions with respect to their argument are obtained directly from the definitions of the respective functions

$$\frac{\mathrm{d}}{\mathrm{d}u}(\mathrm{sn}\, u) = \mathrm{cn}\, u\, \mathrm{dn}\, u, \quad \frac{\mathrm{d}}{\mathrm{d}u}(\mathrm{cn}\, u) = -\mathrm{sn}\, u\, \mathrm{dn}\, u, \quad \frac{\mathrm{d}}{\mathrm{d}u}(\mathrm{dn}\, u) = -k^2 \mathrm{sn}\, u\, \mathrm{cn}\, u.$$

Let us also notice that in the case of $\zeta = 1$, respectively $\varphi = \pi/2$, the integrals (14) – (16) are said to be the *complete elliptic integrals* of the respective kind which are denoted as

$$K(k) = F(\pi/2, k), \quad E(k) = E(\pi/2, k), \quad \Pi(n, k) = \Pi(\pi/2, n, k). \tag{23}$$

In order to proceed with the canonization of the integral (10), we need to know the roots of the quadratic polynomial (13), and in what order the roots, when they are real, are related to each other and the number one, which is the third root of the polynomial under the radical $\sqrt{(1-t)P(t)}$. Depending on the sign of the discriminant

$$\mathcal{D} = (\nu - 1)^3(\nu - 9)$$

the roots of $P(t)$

$$\sigma = \frac{\nu - 1}{8}\left(\nu - 5 + \sqrt{(\nu-1)(\nu-9)}\right), \quad \tau = \frac{\nu - 1}{8}\left(\nu - 5 - \sqrt{(\nu-1)(\nu-9)}\right) \tag{24}$$

may be either real, for $\nu \in (-\infty, 1] \cup [9, +\infty)$ or complex, for $\nu \in (1, 9)$. The real roots are positive numbers, $\sigma > 0$, $\tau > 0$, and when $\sigma \neq \tau$ (simple roots), either $\sigma < \tau$, for $\nu \in (-\infty, 1)$, or $\tau < \sigma$, for $\nu \in (9, +\infty)$. A more precise reasoning

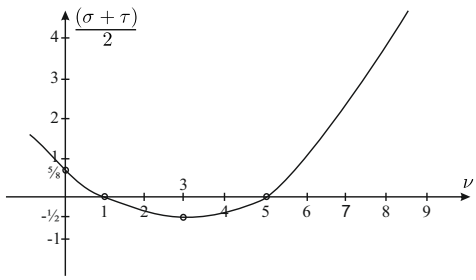

Figure 4. Graphic of the arithmetic mean of the roots of the polynomial $P(t)$ versus ν.

reveals that in the case of simple roots there are exactly three possibilities for the number one: to be the smallest $1 < \tau < \sigma$, the largest $\sigma < \tau < 1$, or between the other two, i.e., $\sigma < 1 < \tau$.

All of the above statements can be proven by inspection relying on the arithmetic mean of the roots σ and τ versus ν

$$\frac{1}{2}(\sigma + \tau) = \frac{1}{8}(\nu - 1)(\nu - 5)$$

and the observation that the sign of $P(1) = 4\,\nu$ alternates while the sign of $P(0) = (\nu - 1)^2$ is always positive (cf. the graphic in Fig. 4). Consequently, there are four specific ranges of the values of the parameter ν, related to the four possible ranges of the roots of the polynomial under the radical $\sqrt{(1-t)P(t)}$

$$\begin{array}{rll} \mathcal{S}^{\mathrm{I}}(\nu) & \nu \in (-\infty, 0), & 0 < \sigma_1 < 1 < \tau_1 \\ \mathcal{S}^{\mathrm{II}}(\nu) & \nu \in (0, 1), & 0 < \sigma_2 < \tau_2 < 1 \\ \mathcal{S}^{\mathrm{III}}(\nu) & \nu \in (1, 9), & \sigma_3 \in \mathbb{C},\ \tau_3 \in \mathbb{C} \\ \mathcal{S}^{\mathrm{IV}}(\nu) & \nu \in (9, +\infty), & 1 < \tau_4 < \sigma_4. \end{array} \tag{25}$$

As a result the whole set of non-bending surfaces are split up into four *classes of surfaces* $\mathcal{S}^{\mathrm{I}}(\nu)$ - $\mathcal{S}^{\mathrm{IV}}(\nu)$ that differ by the range of the values of the parameter ν (cf. Fig. 5). Our next goal is to present the canonical parameterizations of the surfaces in each one of these classes by using the normal forms of the elliptical integrals and the Jacobian elliptic functions.

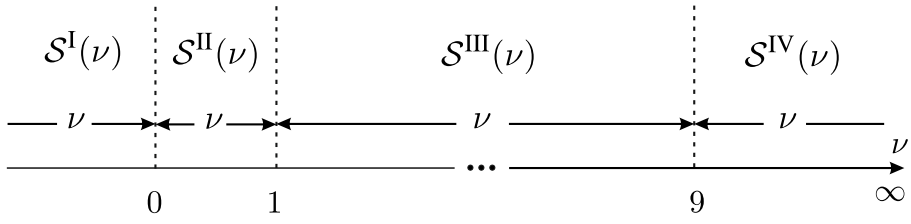

Figure 5. Ranges of the variable ν related to the different classes of non-bending surfaces.

We start with some observations regarding the general properties of the considered non-bending surfaces. For the integral (10) to be defined the polynomial $P(t)$ must obey some constraints. In the range of integration (11), i.e., for the surfaces lying inside the cylinder, the values of the polynomial have to be positive

$$P(t) > 0, \qquad t \in (0, 1)$$

and in the range of integration (12), i.e., for the surfaces that are outside the cylinder, the values of the polynomial have to be negative

$$P(t) < 0, \qquad t \in (1, +\infty).$$

Under such constraints, as it is easily seen from the suggestive graphics in Fig. 6, it follows that the first two classes of non-bending surfaces consist of open "at the top" surfaces, lying either outside the cylinder, if they are surfaces in $\mathcal{S}^{\mathrm{I}}(\nu)$ class

$$\mathcal{S}^{\mathrm{I}}(\nu): \qquad x \in [r, r\sqrt{\tau_1}], \qquad \chi \in [1, \tau_1], \qquad t \in (1, \tau_1) \tag{26}$$

or inside the cylinder, if they are surfaces from $\mathcal{S}^{\mathrm{II}}(\nu)$

$$\begin{aligned} \mathcal{S}^{\mathrm{II}}(\nu): \qquad & x \in [r\sqrt{\tau_2}, r], \qquad \chi \in [\tau_2, 1], \qquad t \in (\tau_2, 1). \\ & P(t) < 0, \qquad t \in (1, +\infty). \end{aligned} \tag{27}$$

All of the non-bending surfaces belonging to the classes $\mathcal{S}^{\mathrm{III}}(\nu)$ and $\mathcal{S}^{\mathrm{IV}}(\nu)$ are closed and they are lying inside the cylinder, i.e.,

$$\mathcal{S}^{\mathrm{III}}(\nu) \text{ and } \mathcal{S}^{\mathrm{IV}}(\nu): \qquad x \in [0, r], \qquad \chi \in [0, 1], \qquad t \in (0, 1). \tag{28}$$

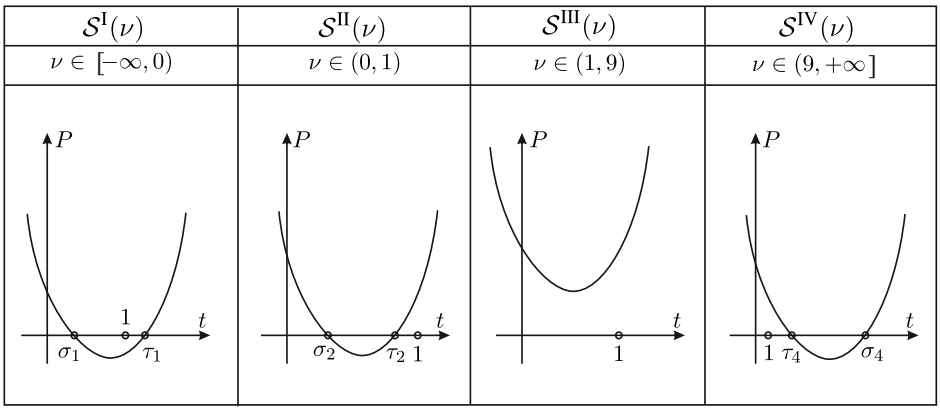

Figure 6. Graphics of the polynomial $P(t)$ related to the different classes of non-bending surfaces.

Thus the whole set of the non-bending surfaces are divided into two subsets of open and closed surfaces, obtained respectively, for $\nu < 1$ and $\nu \geq 1$ (Fig. 7, right). As mentioned already in the Introduction, Gurevich and Kalinin [7] have arrived at the same conclusion relying on numerical and graphical representations. In a difficult to access thesis from 1983, Cherdantzev [4] had succeeded in finding analytical expressions for some of the classes introduced here in terms of the elliptic integrals but makes the wrong assertion that this is not possible for all of them.

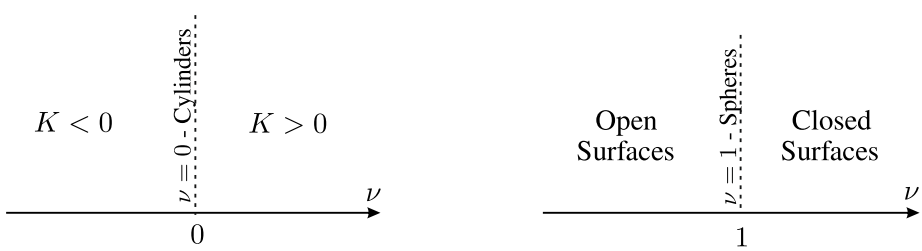

Figure 7. Ranges of the variable ν related to the non-bending surfaces with negative and positive Gaussian curvature (left), and open and closed surfaces (right).

Bellow we will derive not one but three different parameterizations for each class having in mind their future applications. Unfortunately, the comparison with the results in [4] is not so easy because there the author had made use of a different parameter, i.e., ν^{-1} which makes the task quite difficult. It is a challenging problem however to do these checks via the present day Computer Algebra Systems like `Maple` and `Mathematica`.

3. Non-Bending Surfaces of the First Class $\mathcal{S}^{\mathrm{I}}(\nu)$

As shown above, the non-bending surfaces of the first class (for $\nu \in [-\infty, 0)$, cf. Fig. 5) are open "at the top" surfaces (with the exception of the "degenerate surface" $\nu = -\infty$) lying outside the cylinder $\nu = 0$, whose profile curves (upper right parts), according to the equation (10) are given by the formula

$$z_1(\chi) = \frac{r}{2} \int\limits_1^{\chi} \frac{t\mathrm{d}t}{\sqrt{(1-t)(t-\sigma_1)(t-\tau_1)}}, \qquad \chi = \frac{x^2}{r^2}, \qquad x \in [r, r\sqrt{\tau_1}] \quad (29)$$

where the roots σ_1 and τ_1, calculated by the equations (24) for $\nu \in (-\infty, 0)$, are such that the following inequalities hold (compare with the first item in (25) and (26))

$$0 < \sigma_1 < 1 < t < \tau_1, \qquad 0 < \sigma_1 < 1 \le \chi \le \tau_1. \quad (30)$$

To this class of open surfaces we add also the limiting case $\nu = -\infty$, which actually is a "degenerate open surface" being part of the coordinate plane $z = 0$ complimentary to the right circular disk with radius r centered at the origin of this plane.

On substituting with

$$t = 1 + \xi^2, \qquad \chi = 1 + \tilde{\chi}^2, \qquad \xi > 0, \qquad \tilde{\chi} \ge 0$$

the polynomial under the radical in (29) is transformed to a product of a sum and a difference of squares

$$z_1(\tilde{\chi}) = r \int\limits_0^{\tilde{\chi}} \frac{(1+\xi^2)\mathrm{d}\xi}{\sqrt{(\tilde{\sigma}_1^2 + \xi^2)(\tilde{\tau}_1^2 - \xi^2)}}, \quad \tilde{\chi} = \sqrt{\frac{x^2}{r^2} - 1}, \quad x \in [r, r\sqrt{\tau_1}] \quad (31)$$

where

$$\tilde{\sigma}_1 = \sqrt{1-\sigma_1}, \qquad \tilde{\tau}_1 = \sqrt{\tau_1 - 1}, \qquad 0 < \xi < \tilde{\tau}_1, \qquad 0 \leq \tilde{\chi} \leq \tilde{\tau}_1.$$

This latter integral can be split into two integrals

$$\int\limits_0^{\tilde{\chi}} \frac{(1+\xi^2)\mathrm{d}\xi}{\sqrt{(\tilde{\sigma}_1^2+\xi^2)(\tilde{\tau}_1^2-\xi^2)}} = \int\limits_0^{\tilde{\tau}_1} \frac{(1+\xi^2)\mathrm{d}\xi}{\sqrt{(\tilde{\sigma}_1^2+\xi^2)(\tilde{\tau}_1^2-\xi^2)}} - \int\limits_{\tilde{\chi}}^{\tilde{\tau}_1} \frac{(1+\xi^2)\mathrm{d}\xi}{\sqrt{(\tilde{\sigma}_1^2+\xi^2)(\tilde{\tau}_1^2-\xi^2)}}$$

each of which is obtained as a special case of the elliptic integral

$$\int\limits_{\zeta}^{\tilde{\tau}_1} \frac{(1+\xi^2)\mathrm{d}\xi}{\sqrt{(\tilde{\sigma}_1^2+\xi^2)(\tilde{\tau}_1^2-\xi^2)}}, \qquad 0 \leq \zeta < \tilde{\tau}_1 \tag{32}$$

with $\zeta = 0$ and $\zeta = \tilde{\chi}$, respectively. The integral (32) can be reduced to its canonical form with the help of the Jacobian cosine elliptic function, replacing ξ and ζ by the new variables $\tilde{u}$ and u

$$\xi = \tilde{\tau}_1 \mathrm{cn}(\tilde{u}, k_1), \quad \zeta = \tilde{\tau}_1 \mathrm{cn}(u, k_1), \quad u = F(\varphi(\zeta), k_1), \quad u \in (0, K(k_1)] \tag{33}$$

thereby employing the "inversion procedure" illustrated by the commutative diagram in Fig. 8. where

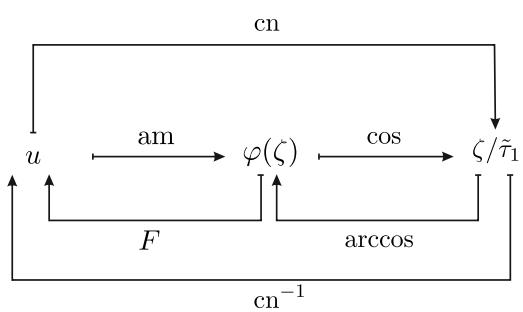

Figure 8. Commutative diagram illustrating the "inversion procedure" for the canonization of the elliptic integral (32).

$$\varphi(\zeta) = \arccos\left(\frac{\zeta}{\tilde{\tau}_1}\right), \qquad k_1 = \frac{\tilde{\tau}_1}{\sqrt{\tilde{\sigma}_1^2+\tilde{\tau}_1^2}}. \tag{34}$$

Hence, the reduction of the elliptic integral (32) follows in succession

$$\int\limits_{\zeta}^{\tilde{\tau}_1} \frac{(1+\xi^2)\mathrm{d}\xi}{\sqrt{(\tilde{\sigma}_1^2+\xi^2)(\tilde{\tau}_1^2-\xi^2)}} = \int\limits_{0}^{u} \frac{(1+\tilde{\tau}_1^2\,\mathrm{cn}^2\tilde{u})\mathrm{dn}\,\tilde{u}\,\mathrm{d}\tilde{u}}{\sqrt{\tilde{\sigma}_1^2+\tilde{\tau}_1^2-\tilde{\tau}_1^2\,\mathrm{sn}^2\tilde{u}}}$$

$$= \frac{1}{\sqrt{\tilde{\sigma}_1^2+\tilde{\tau}_1^2}} \int\limits_{0}^{u} \frac{(1+\tilde{\tau}_1^2\,\mathrm{cn}^2\tilde{u})\mathrm{dn}\,\tilde{u}\,\mathrm{d}\tilde{u}}{\sqrt{1-k_1^2\,\mathrm{sn}^2\tilde{u}}} = \frac{1}{\sqrt{\tilde{\sigma}_1^2+\tilde{\tau}_1^2}} \Big(\int\limits_{0}^{u} \mathrm{d}\tilde{u} + \tilde{\tau}_1^2 \int\limits_{0}^{u} \mathrm{cn}^2\tilde{u}\mathrm{d}\tilde{u} \Big)$$

$$= \frac{1}{\sqrt{\tilde{\sigma}_1^2+\tilde{\tau}_1^2}} \Big(\int\limits_{0}^{u} \mathrm{d}\tilde{u} + \frac{\tilde{\tau}_1^2}{k_1^2} \Big(\int\limits_{0}^{u} \mathrm{dn}^2\tilde{u}\mathrm{d}\tilde{u} - (1-k_1^2) \int\limits_{0}^{u} \mathrm{d}\tilde{u} \Big) \Big) \tag{35}$$

$$= \frac{1}{k_1^2\sqrt{\tilde{\sigma}_1^2+\tilde{\tau}_1^2}} \Big(\Big(k_1^2 - (1-k_1^2)\tilde{\tau}_1^2 \Big) F(\varphi(\zeta),k_1) + \tilde{\tau}_1^2 E(\varphi(\zeta),k_1) \Big).$$

In the above chain of equalities we have made use of the fundamental relations between the Jacobian elliptic functions (19), the normal elliptic integrals (20) – (22) and the formula for the differentiation of the Jacobian cosine function (see above in Section 2). On returning back to the profile curve (31), we make two substitutions in the last line of (35), $\zeta = 0$ and $\zeta = \tilde{\chi}$, and then, by subtracting the obtained expressions, we are led to the canonical form (cf. [1, Formula (213.13)])

$$z_1(\tilde{\chi}) = \frac{r}{k_1^2\sqrt{\tilde{\sigma}_1^2+\tilde{\tau}_1^2}} \Big((k_1^2 - (1-k_1^2)\tilde{\tau}_1^2) \big(K(k_1) - F(\varphi(\tilde{\chi}),k_1) \big) + \tilde{\tau}_1^2 \big(E(k_1) - E(\varphi(\tilde{\chi}),k_1) \big) \Big), \qquad \tilde{\chi} = \sqrt{\frac{x^2}{r^2}-1}, \qquad x \in [r, r\sqrt{\tau_1}]$$

where the complete elliptic integrals $K(k_1)$ and $E(k_1)$ are obtained from the incomplete ones with argument $\varphi(0) = \pi/2$ (cf. equations (23) and (34)).

Written with the help of the variable x the above expression provides the explicit parameterization of the profile curves of the surfaces from the first class in Monge representation

$$z_1(x) = \frac{r}{\sqrt{\tau_1-\sigma_1}} \Big(\sigma_1 \Big(K(k_1) - F(\varphi(x),k_1) \Big) + (\tau_1-\sigma_1) \Big(E(k_1) - E(\varphi(x),k_1) \Big) \Big) \tag{36}$$

$$\varphi(x) = \arccos\sqrt{\frac{(x/r)^2-1}{\tau_1-1}}, \qquad k_1 = \sqrt{\frac{\tau_1-1}{\tau_1-\sigma_1}}, \qquad x \in [r, r\sqrt{\tau_1}]$$

where σ_1 and τ_1 are calculated by (24) for each one of the surfaces with a parameter $\nu \in (-\infty, 0)$. Note that the above formula describes only the upper right part of the profile curve. The whole curve is obtained by two consecutively applied reflections with respect to the coordinate axes OX and OZ (cf. Fig. 2).

The next two canonical representations of the surfaces of the first class are obtained from (36) by introducing two real parameters. One of these parameters v coincides with the angular coordinate ϕ of the meridians (Fig. 1). The other parameter u is related to $\tilde{\chi}$ (respectively to the coordinate x) in two different ways, either by the equations

$$u = \operatorname{arccsc}\sqrt{1+\tilde{\chi}^2} = \operatorname{arccsc}\left(\frac{x}{r}\right), \qquad u \in \left[\operatorname{arccsc}\sqrt{\tau_1},\ \frac{\pi}{2}\right] \tag{37}$$

or by the equations

$$u = \operatorname{cn}^{-1}\Big(\frac{\tilde{\chi}}{\tilde{\tau}_1}\Big) = \operatorname{cn}^{-1}\Big(\sqrt{\frac{(x/r)^2-1}{\tau_1-1}}\Big), \qquad u \in [0,\ 2K(k_1)]\,. \tag{38}$$

The corresponding canonical representations of the non-bending surfaces of the first class, i.e., of the surfaces obtained for $\nu \in (-\infty, 0)$ (excluding the degenerate surface $\nu = -\infty$) are given either by the set of equations

$$\begin{gathered}
z_1(u) = r\left(\frac{1+\lambda_1^2-\mu_1^2}{\mu_1}\Big(K(k_1)-F(\varphi(u),k_1)\Big)+\mu_1\Big(E(k_1)-E(\varphi(u),k_1)\Big)\right)\\
\lambda_1 = \frac{\sqrt{(1-\delta)\nu^2-(6-\delta)\nu-3}}{2\sqrt{2}}, \qquad \mu_1 = \frac{\sqrt{(1-\nu)\delta\nu}}{2}, \qquad k_1 = \frac{\lambda_1}{\mu_1}\\
\delta = \frac{\sqrt{(\nu-1)(\nu-9)}}{\nu}, \quad \varphi(u) = \arccos\Big(\frac{\cot u}{\lambda_1}\Big), \quad \beta = \operatorname{arccsc}\sqrt{1+\lambda_1^2}\\
x(u,v) = r\csc u\,\cos v, \quad y(u,v) = r\csc u\,\sin v, \quad z(u,v) = z_1(u), \quad u \in \left[\beta,\ \frac{\pi}{2}\right]
\end{gathered} \tag{39}$$

or by another set of formulas in which appears the same parameter u running however in a different interval, i.e.,

$$\begin{gathered}
x_1(u) = r\sqrt{1+\lambda_1^2\operatorname{cn}^2 u}, \qquad u \in [0,\ 2K(k_1)]\,, \qquad v \in [0, 2\,\pi]\\
z_1(u) = r\left(\frac{1+\lambda_1^2-\mu_1^2}{\mu_1}\Big(K(k_1)-u\Big)+\mu_1\Big(E(k_1)-E(\operatorname{am} u,k_1)\Big)\right)\\
x(u,v) = x_1(u)\cos v, \qquad y(u,v) = x_1(u)\sin v, \qquad z(u,v) = z_1(u)
\end{gathered} \tag{40}$$

where λ_1, μ_1 and k_1 are defined in (39). Notice that both parameterizations rely on the same axial variable $v \in [0, 2\,\pi]$.

Using one and the same notation u for parameters with different meanings and different ranges deserve some explanation. Such use allows different parameterizations to be represented in an uniformed way which generally does not lead to confusion. But nevertheless one must be careful not to confuse the parameter u in the representation (37) with the variable u that has been previously used for denoting the values of the normal elliptic integral of the first kind (cf. (20)). In the same time the variable u in the representation (38) appears in exactly that previous meaning, related here with the inverse of the Jacobian cosine function. The latter becomes at once transparent if one looks at the commutative diagram in Fig. 8 with the variable ζ replaced by $\tilde{\chi}$.

It should be noted that for the parameterization (39), in the indicated interval of the parameter u, only that part of the surface $\mathcal{S}$ which is over the XOY-plane (the upper half part) can be obtained. For both the parameterizations (39) and (40) the profile curve of the shell is traced from north to south. Graphics of the profile curves of some surfaces of the first class are given in Fig. 9.

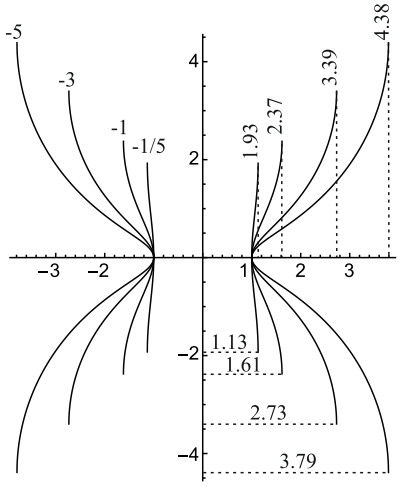

Figure 9. Plots of the profiles curves of non-bending surfaces of the first class for $\nu = -\frac{1}{5}$, -1, -3, -5 (from inner to the outer surfaces).

4. Non-Bending Surfaces of the Second Class $\mathcal{S}^{\mathrm{II}}(\nu)$

As shown in Section 2, the non-bending surfaces in the second class (generated with $\nu \in (0,1)$, cf. Fig. 5) are open "at the top" and lie inside the cylinder $\nu = 0$. According to the equation (10) and the condition (11), their profile curves (upper right parts) are given by

$$z_2(\chi) = \frac{r}{2}\int\limits_{\chi}^{1} \frac{t\mathrm{d}t}{\sqrt{(1-t)(t-\sigma_2)(t-\tau_2)}}, \qquad \chi = \frac{x^2}{r^2}, \qquad x \in [r\sqrt{\tau_2}, r] \quad (41)$$

where the roots σ_2 and τ_2, calculated for $\nu \in (0,1)$ by the equations (24), are such that the following inequalities hold (cf. the second item in (25) and (27))

$$0 < \sigma_2 < \tau_2 < t < 1, \qquad 0 < \sigma_2 < \tau_2 \leq \chi \leq 1. \quad (42)$$

The reduction of the above elliptic integral goes through the "inversion procedure",

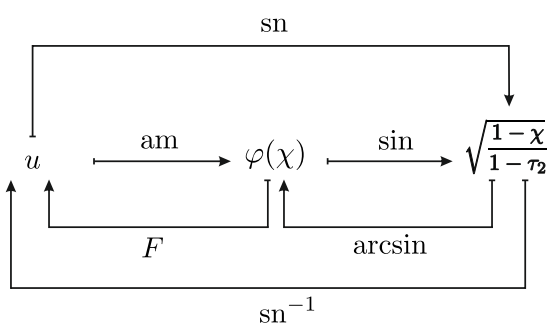

Figure 10. Commutative diagram illustrating the "inversion procedure" for the canonization of the elliptic integral (41).

as illustrated by the commutative diagram in Fig. 10, on writing

$$t = 1 - (1-\tau_2)\mathrm{sn}^2(\tilde{u}, k_2), \qquad \chi = 1 - (1-\tau_2)\mathrm{sn}^2(u, k_2) \quad (43)$$

where

$$u = F(\varphi(\chi), k_2), \qquad \varphi(\chi) = \mathrm{arcsin}\sqrt{\frac{1-\chi}{1-\tau_2}}, \qquad k_2 = \sqrt{\frac{1-\tau_2}{1-\sigma_2}}. \quad (44)$$

By substituting and integrating in succession the profile curve in (41) is reduced to a representation involving only normal elliptic integrals of the first and the second kind (cf. [1, Formula (236.20)])

$$z_2(\chi) = \frac{r}{2}\int\limits_{\chi}^{1} \frac{t\mathrm{d}t}{\sqrt{(1-t)(t-\sigma_2)(t-\tau_2)}} = r\int\limits_{0}^{u} \frac{\big(1-(1-\tau_2)\mathrm{sn}^2\tilde{u}\big)\,\mathrm{dn}\,\tilde{u}\,\mathrm{d}\tilde{u}}{\sqrt{1-\sigma_2-(1-\tau_2)\mathrm{sn}^2\tilde{u}}}$$

$$= \frac{r}{\sqrt{1-\sigma_2}}\int\limits_{0}^{u} \frac{(1-(1-\tau_2)\mathrm{sn}^2\tilde{u})\mathrm{dn}\,\tilde{u}\,\mathrm{d}\tilde{u}}{\sqrt{1-k_2^2\,\mathrm{sn}^2\tilde{u}}} = \frac{r}{\sqrt{1-\sigma_2}}\int\limits_{0}^{u}\Big(1-(1-\tau_2)\mathrm{sn}^2\tilde{u}\Big)\mathrm{d}\tilde{u}$$

$$= \frac{r}{\sqrt{1-\sigma_2}}\Big(\int\limits_{0}^{u}\mathrm{d}\tilde{u} - \frac{1-\tau_2}{k_2^2}\Big(\int\limits_{0}^{u}\mathrm{d}\tilde{u} - \int\limits_{0}^{u}\mathrm{dn}^2\tilde{u}\,\mathrm{d}\tilde{u}\Big)\Big) \tag{45}$$

$$= \frac{r}{\sqrt{1-\sigma_2}}\Big(\sigma_2 F(\varphi(\chi),k_2) + (1-\sigma_2)E(\varphi(\chi),k_2)\Big).$$

In the above chain of equalities we have made use of the formulas (19) – (22), and as well as, the formula for the derivative of the Jacobian sine elliptic function (refer to Section 2).

On returning back to the variable x in the last line of (45) we arrive at our first explicit parameterization of the profile curves of the surfaces of the second class in Monge representation

$$z_2(x) = \frac{r}{\sqrt{1-\sigma_2}}\Big(\sigma_2 F(\varphi(x),k_2) + (1-\sigma_2)E(\varphi(x),k_2)\Big)$$

$$\varphi(x) = \arcsin\sqrt{\frac{1-(x/r)^2}{1-\tau_2}}, \qquad k_2 = \sqrt{\frac{1-\tau_2}{1-\sigma_2}}, \qquad x\in[r\sqrt{\tau_2}, r] \tag{46}$$

where σ_2 and τ_2 are calculated by (24) for each one of the surfaces with a parameter $\nu\in(0,1)$. Note that the above formula describes only the upper right part of the profile curve. The whole curve is obtained by two consecutively applied reflections with respect to the coordinate axes OX and OZ (cf. Fig. 2).

Now we are going to give two canonical representations of the non-bending surfaces of the second class obtained from (46) by referring to the roots of the polynomial $P(t)$ as functions of ν and substituting for χ with a new parameter u, defined in two different ways, either by the equations

$$u = \arcsin\sqrt{\chi} = \arcsin\left(\frac{x}{r}\right), \qquad u\in\Big[\arcsin\sqrt{\tau_2},\,\frac{\pi}{2}\Big] \tag{47}$$

or by the equations

$$u = \mathrm{sn}^{-1}\Big(\sqrt{\frac{1-\chi}{1-\tau_2}}\Big) = \mathrm{sn}^{-1}\Big(\sqrt{\frac{1-(x/r)^2}{1-\tau_2}}\Big), \quad u\in[-K(k_2),\, K(k_2)]\,. \tag{48}$$

We have two choices for the parameter u, i.e., (47) and (48) with different ranges and relationships with the variable χ (respectively the coordinate x). Their notation should not create however confusion in respective parameterizations of the profile curves. The commutative diagram in Fig. 10 may serve to elucidate the meaning of the second choice.
As a result the corresponding canonical representations of the non-bending surfaces of the second class, i.e., of the surfaces obtained for $\nu \in (0,1)$, are given either by the set of equations

$$\begin{gathered} z_2(u) = r\Big(\frac{1-\mu_2^2}{\mu_2}\,F(\varphi(u),k_2) + \mu_2 E(\varphi(u),k_2)\Big), \qquad k_2 = \frac{\lambda_2}{\mu_2} \\ \lambda_2 = \frac{\sqrt{3+(6-\delta)\nu-(1-\delta)\nu^2}}{2\sqrt{2}}, \qquad \mu_2 = \frac{\sqrt{3+(6+\delta)\nu-(1+\delta)\nu^2}}{2\sqrt{2}} \\ \varphi(u) = \arcsin\left(\frac{\cos u}{\lambda_2}\right), \quad \delta = \frac{\sqrt{(\nu-1)(\nu-9)}}{\nu}, \quad \beta = \arcsin\sqrt{1-\lambda_2^2} \end{gathered} \tag{49}$$

$$x(u,v) = r\sin\!u\,\cos v, \quad y(u,v) = r\sin\!u\,\sin v, \quad z(u,v) = z_2(u), \quad u\in\Big[\beta,\,\frac{\pi}{2}\Big]$$

or by another set of equations in which the parameter u appears again, but this time with a different range, i.e.,

$$\begin{gathered} x_2(u) = r\sqrt{1-\lambda_2^2\,\mathrm{sn}^2\,u}, \qquad z_2(u) = r\Big(\frac{1-\mu_2^2}{\mu_2}\,u + \mu_2 E(\mathrm{am}\,u,k_2)\Big) \\ x(u,v) = x_2(u)\cos v, \qquad y(u,v) = x_2(u)\sin v, \qquad z(u,v) = z_2(u) \end{gathered} \tag{50}$$

where λ_2, μ_2 and the modulus k_2 are defined in (49), $u\in[-K(k_2),\,K(k_2)]$ and $v\in[0,2\,\pi]$.

Notice that the second parameter v, which is the same for both parameterizations, coincides with the angular coordinate of the meridians.
For the parameterization (49), in the indicated interval of the parameter u, only that part of the surface $\mathcal{S}$ which is over the XOY-plane (the upper half part) is

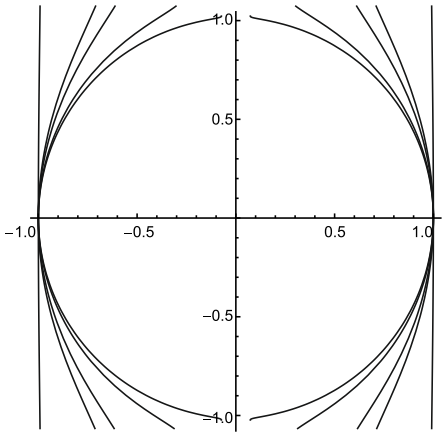

Figure 11. Plots of the profiles curves of non-bending surfaces of the second class drawn with $\nu = 0.99$, 0.93, 0.90, 0.66 and 0 (from inner to the outer surfaces).

obtained. The profile curve of the shell is traced from north to the equator in the first quadrant, in the parameterization (49), and from south through the equator to north in the first and fourth quadrants, in the second parameterization (50) (see Fig. 11).

5. Non-Bending Surfaces of the Third Class $\mathcal{S}^{\mathrm{III}}(\nu)$

The non-bending surfaces of the third class (for $\nu \in (1, 9)$, cf. Fig. 5) are closed surfaces lying inside the cylinder $\nu = 0$ in the space between the sphere $\nu = 1$ and the surface $\nu = 9$, which profile curves (the upper right parts) according to equations (10) – (11) are given by the formula

$$z_3(\chi) = \frac{r}{2} \int\limits_{\chi}^{1} \frac{t\mathrm{d}t}{\sqrt{(1-t)(t-\sigma_3)(t-\tau_3)}}, \qquad \chi = \frac{x^2}{r^2}, \qquad x \in [0, r]. \tag{51}$$

The roots σ_3 and τ_3 of the polynomial $P(t)$, calculated by the equations (24) for $\nu \in (1, 9)$, are complex numbers (compare the third item in (25) and (28)). The reduction of the above integral to normal form relies on the substitutions (cf. [1, Formula (243.00)])

$$t = \frac{1 - A + (1 + A)\mathrm{cn}(\tilde{u}, k_3)}{1 + \mathrm{cn}(\tilde{u}, k_3)}, \qquad \chi = \frac{1 - A + (1 + A)\mathrm{cn}(u, k_3)}{1 + \mathrm{cn}(u, k_3)} \tag{52}$$

where

$$A = \frac{1}{2}\sqrt{(\sigma_3 + \tau_3 - 2)^2 - (\sigma_3 - \tau_3)^2}, \qquad k_3 = \frac{1}{2}\sqrt{2 - \frac{\sigma_3 + \tau_3 - 2}{A}}. \tag{53}$$

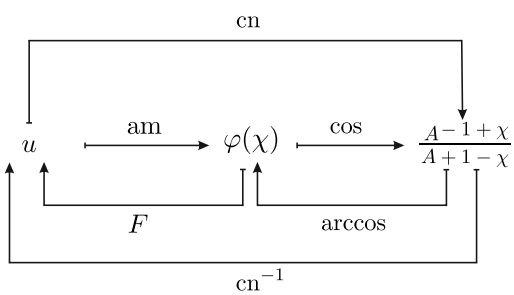

Figure 12. Commutative diagram illustrating the "inversion procedure" for the canonization of the elliptic integral (51).

The commutative diagram in Fig. 12 indicates the fundamental role of the "inversion procedure" in canonizing the integral (51) achieved by introducing the relations

$$u = F(\varphi(\chi), k_3), \qquad \varphi(\chi) = \arccos\Big(\frac{A - 1 + \chi}{A + 1 - \chi}\Big). \tag{54}$$

As a result of performing the above substitutions the following canonical form of the profile curve (51) is obtained

$$\begin{aligned} z_3(\chi) &= \frac{r}{2}\Big(\frac{1 + A}{\sqrt{A}}F(\varphi(\chi), k_3) - 2\sqrt{A}\int_0^u \frac{\mathrm{d}\tilde{u}}{1 + \mathrm{cn}\tilde{u}}\Big) \\ &= \frac{r}{2}\Big(\frac{1 - A}{\sqrt{A}}F(\varphi(\chi), k_3) + 2\sqrt{A}\Big(E(\varphi(\chi), k_3) - \frac{\sin\varphi(\chi)\Delta(\varphi(\chi))}{1 + \cos\varphi(\chi)}\Big)\Big) \end{aligned} \tag{55}$$

in which the standard notation for the *delta* function $\Delta(\varphi) := \sqrt{1 - k_3^2 \sin^2\varphi}$ has been used along with

$$u = \mathrm{cn}^{-1}\Big(\frac{A - 1 + \chi}{A + 1 - \chi}\Big) = \mathrm{cn}^{-1}\Big(\frac{A - 1 + (x/r)^2}{A + 1 - (x/r)^2}\Big), \qquad u \in [-\beta,\, \beta] \tag{56}$$

and

$$\beta = \mathrm{cn}^{-1}\Big(\frac{A - 1}{A + 1}\Big).$$

For additional details of the reduction process, we refer the reader to the Handbook by Byrd and Friedman [1, Formulas (243.07) and (341.53)].

On returning back to the variable x in (55) we obtain the first explicit representation of the profile curves (upper right parts) of the surfaces of the third class

$$z_3(x) = \frac{r}{2\sqrt{A}}\left((1 - A)F(\varphi(x), k_3) + 2A\Big(E(\varphi(x), k_3) - \frac{\sin\varphi(x)\Delta(\varphi(x))}{1 + \cos\varphi(x)}\Big)\right) \tag{57}$$

$$\varphi(x) = \arccos\Big(\frac{A - 1 + (x/r)^2}{A + 1 - (x/r)^2}\Big), \qquad x \in [0, r]$$

where the elliptic modulus k_3 and A are given by (53) and the roots σ_3 and τ_3 are calculated by (24) for the values of the parameter ν in the interval $(1, 9)$.

Let us now introduce a new parameter

$$u = \arcsin\sqrt{\chi} = \arcsin\left(\frac{x}{r}\right), \qquad u \in [-\frac{\pi}{2},\, \frac{\pi}{2}] \tag{58}$$

which, as it is clearly seen from the commutative diagram in Fig. 12, should not be confused with the parameter u used in equations (52) – (55) where it is defined by the formulas (56).

Thus, we have two choices for the parameter u, given by formulas (56) and (58), in which u has different relationships with the variable χ (respectively x). The corresponding canonical representations of the non-bending surfaces of the third class, i.e., of the surfaces obtained for $\nu \in (1, 9)$, are given either by the set of equations

$$z_3(u)=\sqrt[4]{\nu}\,r\Big(\frac{1-\sqrt{\nu}}{2\sqrt{\nu}}F(\varphi(u),k_3)+E(\varphi(u),k_3)-\frac{\sin\varphi(u)\Delta(\varphi(u))}{1+\cos\varphi(u)}\Big)$$

$$\varphi(u)=\arccos\Big(\frac{\sqrt{\nu}-\cos^2 u}{\sqrt{\nu}+\cos^2 u}\Big),\quad k_3=\frac{(1+\sqrt{\nu})\sqrt{(3-\sqrt{\nu})(1+\sqrt{\nu})}}{4\nu^{1/4}} \tag{59}$$

$$x(u,v)=r\sin u\cos v,\quad y(u,v)=r\sin u\sin v,\quad z(u,v)=z_3(u),\quad u\in[-\frac{\pi}{2},\frac{\pi}{2}]$$

or by another set of equations that also involve the parameter u, running however in a different range of values, i.e.,

$$z_3(u)=\sqrt[4]{\nu}\,r\Big(\frac{1-\sqrt{\nu}}{2\sqrt{\nu}}\,u+E(\mathrm{am}\,u,k_3)-\frac{\mathrm{sn}\,u\,\mathrm{dn}\,u}{1+\mathrm{cn}\,u}\Big),\qquad u\in[-\beta,\,\beta]$$

$$x_3(u)=r\sqrt{1-\sqrt{\nu}\frac{1-\mathrm{cn}\,u}{1+\mathrm{cn}\,u}},\qquad \beta=\mathrm{cn}^{-1}(\frac{\sqrt{\nu}-1}{\sqrt{\nu}+1}) \tag{60}$$

$$x(u,v)=x_3(u)\cos v,\quad y(u,v)=x_3(u)\sin v,\quad z(u,v)=z_3(u),\quad v\in[0,2\,\pi]$$

where k_3 is defined in (59) and cn^{-1} is the inverse of the Jacobian cosine function. Note also that the angular parameter v runs over the same range in both parameterizations. For the parameterization (59), in the indicated interval of the parameter u, only that part of the surface $\mathcal{S}$ which is over the XOY-plane (the upper half part) is obtained. The profile curve of the shell in the parameterization (59) is traced clockwise while for the parameterization (60) it is traced counterclockwise (see Fig. 13).

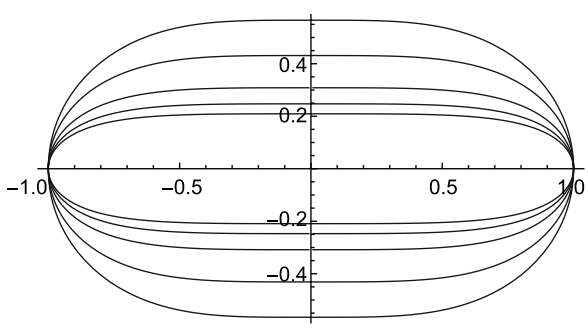

Figure 13. Plots of the profiles curves of non-bending surfaces of the third class for $\nu = 2$, 3, 5, 7 and 9 (from outer to inner surfaces).

6. Non-Bending Surfaces of the Fourth Class $\mathcal{S}^{\mathrm{IV}}(\nu)$

The non-bending surfaces of the fourth class (for $\nu \in (9, +\infty]$, cf. Fig. 5) are closed surfaces lying inside the cylinder $\nu = 0$ in the space enclosed by the surface $\nu = 9$ and the plane $z = 0$ including the plane circular disk with radius r obtained for $\nu = +\infty$. According to equations (10) – (11) their profile curves (upper right parts) are given by the formula

$$z_4(\chi) = \frac{r}{2} \int\limits_{\chi}^{1} \frac{t\mathrm{d}t}{\sqrt{(1-t)(t-\sigma_4)(t-\tau_4)}}, \qquad \chi = \frac{x^2}{r^2}, \qquad x \in [0, r] \tag{61}$$

where the roots σ_4 and τ_4 of the polynomial $P(t)$, calculated by the equations (24) for $\nu \in (9, \infty)$, are such that the following inequalities hold (compare with the fourth item (25) and (28))

$$0 < t < 1 < \tau_4 < \sigma_4, \qquad 0 \leq \chi \leq 1 < \tau_4 < \sigma_4. \tag{62}$$

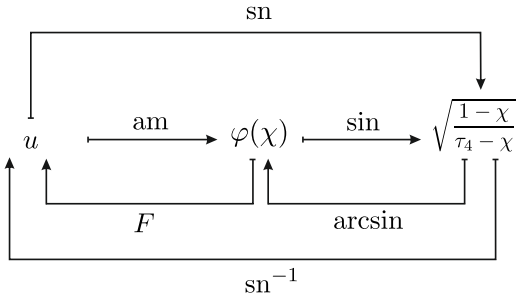

Figure 14. Commutative diagram illustrating the "inversion procedure" for the canonization of the elliptic integral (61).

The reduction of the above elliptic integral goes through the "inversion procedure", as illustrated by the commutative diagram in Fig. 14, on writing

$$t = \mathrm{nc}^2(\tilde{u}, k_4) - \tau_4 \mathrm{tn}^2(\tilde{u}, k_4), \qquad \chi = \mathrm{nc}^2(u, k_4) - \tau_4 \mathrm{tn}^2(u, k_4) \tag{63}$$

$$u = F(\varphi(\chi), k_4), \qquad \varphi(\chi) = \mathrm{arcsin}\sqrt{\frac{1-\chi}{\tau_4 - \chi}}, \qquad k_4 = \sqrt{\frac{\sigma_4 - \tau_4}{\sigma_4 - 1}} \tag{64}$$

where we have used the standard notation $\operatorname{nc} u = 1/\operatorname{cn} u$ and $\operatorname{tn} u = \operatorname{sn} u/\operatorname{cn} u$.

As a result of performing the above substitutions we arrive at the following canonical form

$$z_4(\chi) = \frac{r}{\sqrt{\sigma_4 - 1}}\Big(\int\limits_0^u \operatorname{nc}^2\tilde{u}\,\mathrm{d}\tilde{u} - \tau_4 \int\limits_0^u \operatorname{tn}^2\tilde{u}\,\mathrm{d}\tilde{u}\Big)$$
$$= \frac{r}{\sqrt{\sigma_4 - 1}}\left(F(\varphi(\chi), k_4) - \frac{1-\tau_4}{1-k_4^2}\Big(E(\varphi(\chi), k_4) - \tan\varphi(\chi)\Delta(\varphi(\chi))\Big)\right) \tag{65}$$

in which the standard notation for the *delta* function $\Delta(\varphi) := \sqrt{1 - k_4^2\sin^2\varphi}$ has been used. The rest of the notation are as follows

$$u = \operatorname{sn}^{-1}\Big(\sqrt{\frac{1-\chi}{\tau_4-\chi}}\Big) = \operatorname{sn}^{-1}\Big(\sqrt{\frac{1-(x/r)^2}{\tau_4-(x/r)^2}}\Big), \quad u \in [-\beta,\, \beta]\,, \quad \beta = \operatorname{sn}^{-1}(\frac{1}{\sqrt{\tau_4}})\cdot$$

For additional details of the reduction process, we refer the reader to the Handbook by Byrd and Friedman [1, Formulas (232.19), (313.02) and (316.02)].

On returning back to the variable x in (65) we obtain the first explicit representation of the profile curves (upper right parts) of the surfaces of the fourth class

$$z_4(x) = \frac{r}{\sqrt{\sigma_4 - 1}}\left(F(\varphi(x), k_4) - \frac{1-\tau_4}{1-k_4^2}\Big(E(\varphi(x), k_4) - \tan\varphi(x)\Delta(\varphi(x))\Big)\right) \tag{66}$$

$$\varphi(x) = \arcsin\sqrt{\frac{1-(x/r)^2}{\tau_4-(x/r)^2}}, \qquad k_4 = \sqrt{\frac{\sigma_4-\tau_4}{\sigma_4-1}}, \qquad x \in [0, r]$$

where the roots σ_4 and τ_4 are calculated by (24) for the values of the parameter ν running through the interval $(9, +\infty)$.

Let us now introduce a new parameter

$$u = \arcsin\sqrt{\chi} = \arcsin\left(\frac{x}{r}\right), \qquad u \in [-\frac{\pi}{2},\, \frac{\pi}{2}] \tag{67}$$

which, as it can be seen from the commutative diagram in Fig. 14, should not be confused with the parameter u in equations (63) – (65)

From the above definitions it follows that the two choices of the parameter u have different relationships with the variable χ (respectively x). The corresponding

canonical representations of the non-bending surfaces of the fourth class, i.e., of the surfaces obtained for $\nu \in (9, +\infty)$, are given either by the set of equations

$$
\begin{gathered}
z_4(u) = r\left(\frac{1}{\lambda_4}F(\varphi(u), k_4) + \lambda_4 E(\varphi(u), k_4) - \lambda_4 \tan\varphi(u)\Delta(\varphi(u))\right) \\
\varphi(u) = \arcsin\Big(\frac{2\sqrt{2}\cos u}{\sqrt{(\nu-\delta\nu-5)(\nu-1)-8\sin^2 u}}\Big), \qquad k_4 = \frac{\sqrt{\delta\nu(\nu-1)}}{2\lambda_4} \\
\lambda_4 = \frac{\sqrt{(\delta+1)\nu^2-(\delta+6)\nu-3}}{2\sqrt{2}}, \qquad \delta = \frac{\sqrt{(\nu-1)(\nu-9)}}{\nu} \\
x(u,v) = r\sin u\,\cos v, \quad y(u,v) = r\sin u\,\sin v, \quad z(u,v) = z_4(u), \quad u \in [-\frac{\pi}{2}, \frac{\pi}{2}]
\end{gathered}
\tag{68}
$$

or by another set of equations that also involve the parameter u, running however in a different range of values, i.e.,

$$
\begin{gathered}
x_4(u) = r\sqrt{1-\mu_4^2\,\mathrm{tn}^2\,u}, \qquad z_4(u) = r\Big(\frac{1}{\lambda_4}\,u + \lambda_4 E(\mathrm{am}\,u, k_4) - \lambda_4\,\mathrm{tn}\,u\,\mathrm{dn}\,u\Big) \\
\mu_4 = \frac{\sqrt{(1-\delta)\nu^2-(6-\delta)\nu-3}}{2\sqrt{2}}, \qquad \beta = \mathrm{sn}^{-1}\Big(\frac{1}{\sqrt{\mu_4^2+1}}\Big) \\
x(u,v) = x_4(u)\cos v, \quad y(u,v) = x_4(u)\sin v, \quad z(u,v) = z_4(u), \quad u \in [-\beta,\, \beta]
\end{gathered}
\tag{69}
$$

where δ, λ_4 and the modulus k_4 are defined in (68) and the second parameter $v \in [0, 2\,\pi]$ is the same for both parameterizations. For the parameterization (68), in the indicated interval of the parameter u, only that part of the surface $\mathcal{S}$ which is over the XOY-plane (the upper half part) is obtained. The profile curve of the shell in the parameterization (68) is traced clockwise while for the parameterization (69) it is traced counterclockwise (see Fig. 15).

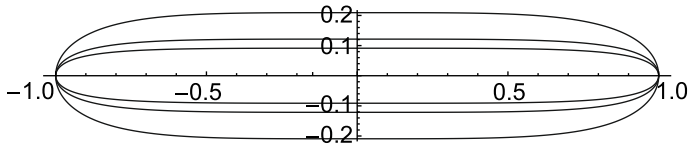

Figure 15. Some plots of the profiles curves of non-bending surfaces of the fourth class for $\nu = 9$, 20 and 50 (from outer to the inner surfaces).

7. Comments

As already mentioned in the Introduction the non-bending condition which is the fundamental for the present considerations is quite different in nature by that considered in the classical differential geometry [9]. One should remind here that the infinitesimal bending $\tilde{\mathcal{S}}$ of the surface $\mathcal{S}$ there is defined by the map $\tilde{\mathbf{x}} : \mathbb{R}^2 \to \mathbb{R}^3$ such that $\tilde{\mathbf{x}} = \mathbf{x} + \varepsilon\mathbf{z}$ in which $\mathbf{x}$ parameterizes $\mathcal{S}$, ε is an infinitesimally small real parameter and $\mathbf{z}$ is a smooth vector field in $\mathbb{R}^3$. The infinitesimal bending is defined locally by the condition

$$\mathrm{d}\tilde{s}^2 - \mathrm{d}s^2 = o(\varepsilon)$$

i.e., the difference of the squares of the line elements of $\mathcal{S}$ and $\tilde{\mathcal{S}}$ is of order higher then the first and this turns out to be equivalent to the system of partial differential equations produced by the vector equation

$$\mathrm{d}\mathbf{x}.\mathrm{d}\mathbf{z} = 0.$$

The nature of the last condition furnishes quite different settings compared to the present considerations. Here we have considered two parametric family of axially symmetric surfaces that can be characterized as Weingarten surfaces which meridional and parallel curvatures satisfy a specific quadratic relationship.
It was found that they form four classes which are split in two sub-classes each of them with two elements consisting of open $\mathcal{S}^{\mathrm{I}}(\nu)$ and $\mathcal{S}^{\mathrm{II}}(\nu)$ or closed $\mathcal{S}^{\mathrm{III}}(\nu)$ and $\mathcal{S}^{\mathrm{IV}}(\nu)$ surfaces. In the frame of the theory of thin-shell structures, such surfaces should have in principle a number of practical applications due to their special "mechanical property" allowing shells of these forms to be deformed without bending. The two characteristic parameters r and ν introduced on the way account respectively for the size and the shape of the surfaces. With a few exceptions generated by $\nu = 0, 1$ and $\nu = 9$ the considered non-bending surfaces have not closed form representations by elementary functions. As a result of a reduction procedure we have succeeded to distinguish four classes which differ by their explicit parameterizations in terms of elliptic integrals and Jacobian elliptic functions. Each one of these classes consists of either closed or "open at the top" surfaces that are lying inside or outside of a right circular cylinder. Two of the surfaces have a degenerate form obtained for $\nu = +\infty$ and $\nu = -\infty$ which are respectively the plane circular disk D_r (r – radius of the disk) and the complementary part $C_r = \mathbb{R}^2 \setminus D_r$ of the plane outside D_r. When the parameter ν changes in the range $\nu \in [-\infty, +\infty]$ the surfaces transform continuously starting from C_r, passing consecutively through the right circular cylinder $\nu = 0$, sphere $\nu = 1$ and ending finally at D_r.

Another interesting fact which should be mentioned is that the north and south poles of all closed surfaces are flat points as there both curvatures κ_π and κ_μ according to their explicit expressions (5) and (6) vanish. Let us remind that the parameter ν was introduced as the ratio κ_μ/κ_π evaluated at the equator E (cf. Fig. 2). It is clear however that this ratio is not the same on the rest of the surface – just

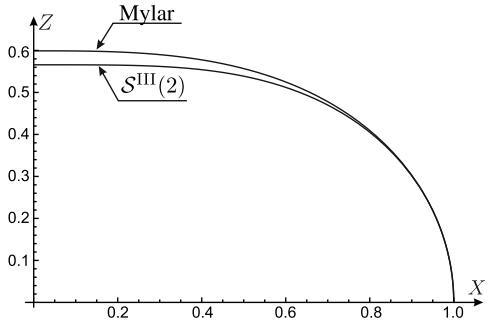

Figure 16. The profiles curves of the Mylar balloon and the non-bending surface from $\mathcal{S}^{\mathrm{III}}(2)$ class with the same radius.

notice that this is governed globally by the Weingarten relationship (2).
There are however two exceptions in which this ratio remains the same along the entire surface $\mathcal{S}$ and these are the sphere ($\nu = 1$) and the surface generated with $\nu = 3$. A remarkable fact is also that never mind with what value of ν we start at the equator we end at the poles with $\kappa_\mu/\kappa_\pi \equiv 3$. This can be seen by checking directly the Weingarten relationship (2) at these points.
It is the right place to mention also that the Mylar balloon is the unique surface (up to a scale) for which the relation $\kappa_\mu = 2\kappa_\pi$ is satisfied globally [14, 15]. Its Aspect Ratio, i.e., the height vs the width of the surface has be found to be 0.59907. Evaluation the same quantity (using formulas (57)) for the surfaces in $\mathcal{S}^{\mathrm{III}}(2)$ class produces 0.56582. In Fig. 16 we have illustrated the difference in the profiles of the Mylar balloon and surfaces in $\mathcal{S}^{\mathrm{III}}(2)$ class.
There are a lot of other issues concerning the non-bending surfaces which deserve comments but we will postpone them for the moment and hope that we will have another chance to do this elsewhere.

References

[1] Byrd P. and Friedman M., *Handbook of Elliptic Integrals for Engineers and Scientists*, 2nd Edn, Springer, New York 1971.

[2] Castro I. and Castro-Infantes I., *Plane Curves with Curvature Depending on the Distance to a Line*, Diff. Geom. Appl. **44** (2016) 77-97.

[3] Castro I., Castro-Infantes I. and Castro-Infantes J., *New Plane Curves with Curvature Depending on Distance from the Origin*, Mediterr. J. Math. (2017) 14: 108. doi:10.1007/s00009-017-0912-z.

[4] Cherdantzev N., *Stability of Non-Bending Ship Shells of Revolution Loaded by Uniform Pressure*, PhD Thesis, Leningrad 1983.

[5] Flügge W., *Stresses in Shells*, Springer, Berlin 1960.

[6] Ganchev G. and Mihova V., *On the Invariant Theory of Weingarten Surfaces in Euclidean Space*, J. Phys. A: Math. & Theor. **43** (2010) 405210-1-27.

[7] Gurevich V. and Kalinin V., *Forms of Shells of Revolution Deforming Without Bending Under Uniform Pressure*, DAN AN SSSR **256** (1981) 1085-1088.

[8] Hertrich-Jeromin U., Mundilova K. and Tjaden E.-H., *Channel Linear Weingarten Surfaces*, J. Geom. Symmetry Phys. **40** (2015) 25-33.

[9] Ivanova-Karatopraklieva I., *Infinitesimal Bending of Higher Order of Rotational Surfaces with a Planar Pole*, Serdica **18** (1992) 59-78.

[10] Krivoshapko S. and Ivanov V., *Encyclopedia of Analytical Surfaces*, Springer, Cham 2015.

[11] Lopez R., *On Linear Weingarten Surfaces*, Int. J. Math. **19** (2008) 439-448.

[12] Lopez R., *Special Weingarten Surfaces Foliated by Circles*, Monatsh Math **154** (2008) 289-302.

[13] Mladenov I. and Hadzhilazova M., *The Many Faces of Elastica*, Springer, Cham 2017.

[14] Mladenov I. and Oprea J., *The Mylar Ballon*: *New Viewpoints and Generalizations*, Geom. Integrability & Quantization **8** (2007) 246-263.

[15] Mladenov I., *On the Geometry of the Mylar Balloon*, C. R. Bulg. Acad. Sci. **54** (2001) 39-44.

[16] Novozhilov V., *Thin Shell Theory*, Noordhoff, Groningen 1964.

[17] Oprea J., *Differential Geometry and Its Applications*, 2nd Edn, Prentice Hall, Upper Saddle River 2003.

[18] Pampano A., *Planar p-Elasticae and Rotational Linear Weingarten Surfaces*, Geom. Integrability & Quantization **20** (2019) 227-238.

[19] Pulov V., Hadzhilazova M. and Mladenov I., *On a Class of Linear Weingarten Surfaces*, Geom. Integrability & Quantization **19** (2018) 168–187.

[20] Pulov V., Hadzhilazova M. and Mladenov I., *Deformations Without Bending*: *Explicit Examples*, Geom. Integrability & Quantization **20** (2019) 246–254.

[21] Toda M., *Weingarten Surfaces with Moving Frames - A Tribute to S. S. Chern and C. L. Terng - And A Duality Result*, JP Journal of Geometry and Topology **12** (2012) 263-289.

Vladimir I. Pulov
Department of Physics
Technical University of Varna
Varna 9010, BULGARIA
E-mail address: vpulov@hotmail.com

Ivaïlo M. Mladenov
Institute of Biophysics
Bulgarian Academy of Sciences
Acad. G. Bonchev Str., Bl. 21
1113 Sofia, BULGARIA
E-mail address: mladenov@bio21.bas.bg